HHS Public Access

Author manuscript

Atherosclerosis. Author manuscript; available in PMC 2024 December 01.

Published in final edited form as:

Atherosclerosis. 2023 December ; 387: 117383. doi:10.1016/j.atherosclerosis.2023.117383.

Macrophage-Restricted Overexpression of Glutaredoxin 1 Protects Against Atherosclerosis by Preventing Nutrient Stress-Induced Macrophage Dysfunction and Reprogramming

Yong Joo Ahn[1,2], **Luxi Wang**[2], **Seonwook Kim**[3], **Matthew R. Eber**[3], **Alessandro G. Salerno**[3], **Reto Asmis**[3,*]

[1]Department of Convergence IT Engineering, School of Convergence Science and Technology, Medical Science and Engineering Program, Pohang University of Science and Technology (POSTECH),

[2]Department of Physiology of the School of Basic Medical Science at Zhejiang University,

[3]Department of Internal Medicine, Wake Forest School of Medicine

Abstract

Background and Aims: Deficiency in the thiol transferase glutaredoxin 1 (Grx1) in aging mice promotes in a sexually dimorphic manner the dysregulation of macrophages and atherogenesis. However, the underlying mechanisms were not known. Here we tested the hypothesis that macrophage-restricted overexpression of Grx1 protects atherosclerosis-prone mice against macrophage reprogramming and dysfunction induced by a high-calorie diet (HCD) and thereby reduce the severity of atherosclerosis.

Methods: We generated lentiviral vectors carrying CD68 promoter-driven EGFP or Grx1 constructs and conducted bone marrow (BM) transplantation studies to overexpress Grx1 in a macrophage-specific manner in male and female atherosclerosis-prone LDLR$^{-/-}$ mice and fed these mice a HCD to induce atherogenesis. Atherosclerotic lesion size was determined in both the aortic root and the aorta. We isolated BM-derived macrophages (BMDM) to assess protein *S*-glutathionylation levels and loss of MKP-1 activity as measures of HCD-induced thiol oxidative

[*]**Address for Correspondence:** Reto Asmis, Wake Forest School of Medicine, Medical Center Boulevard, Winston-Salem; Tel.: (336) 713-7521, rasmis@wakehealth.edu.

Author Contributions

Y.J.A., L.W, and SK performed experiments and contributed significantly to the preparation of the manuscript. A.S and M.E assisted with the experiments and data analysis and contributed to the editing of the manuscript. R.A. provided funding, designed the experiments, wrote the manuscript, generated the figures and contributed to the editing of the manuscript.

Conflict of Interest

The authors declare that they have no known competing financial interests or personal relationships that could have appeared to influence the work reported in this paper.

Submission Declaration Statement

The authors declare that this manuscript, or part of it, has neither been published nor is currently under consideration for publication by any other journal. All authors have read the manuscript and approved its submission to Arteriosclerosis.

stress. We also conducted gene profiling on these BMDM to determine the impact of Grx1 activity on HCD-induced macrophage reprogramming.

Results: Overexpression of Grx1 protected macrophages against HCD-induced protein *S*-glutathionylation, reduced monocyte chemotaxis *in vivo*, limited macrophage recruitment into atherosclerotic lesions, and was sufficient to reduce the severity of atherogenesis in both male and female mice. Gene profiling revealed major sex differences in the transcriptional reprogramming of macrophages induced by HCD feeding, but Grx1 overexpression only partially reversed HCD-induced transcriptional reprogramming of macrophages.

Conclusions: Macrophage Grx1 plays a major role in protecting mice atherosclerosis mainly by maintaining the thiol redox state of the macrophage proteome and preventing macrophage dysfunction.

Graphical Abstract:

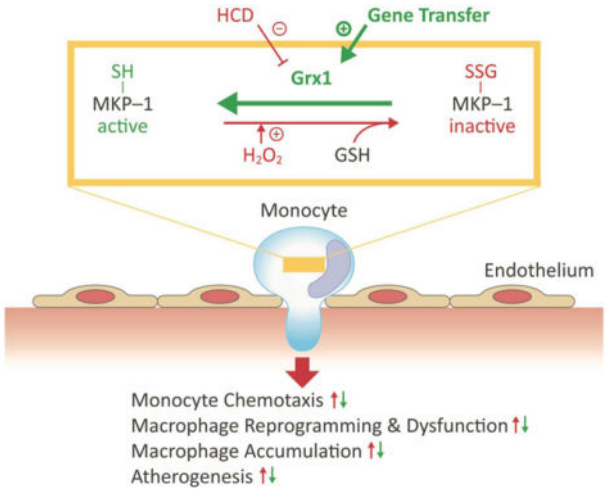

Overexpression of Grx1 protects against Atherogenesis by preventing HCD-induced Protein S-Glutathionylation of the Macrophage Proteome, Macrophage and Thereby Protecting Macrophages from Reprogramming and Dysfunction. HCD feeding of mice promotes the *S*-glutathionylation of the macrophage proteome, including MKP-1, a master regulator of monocyte and macrophage function and activation. MKP-1 is inactivated and degraded upon *S*-glutathionylation, resulting in enhanced monocyte chemotaxis, increased recruitment of reprogrammed and dysfunctional MDM, and accelerated atherogenesis. Overexpression of Grx1 in macrophages preserves their protein thiol redox state, normalizes monocyte chemotaxis, and reduces macrophages accumulation and atherosclerotic lesion formation.

Keywords

atherosclerosis; glutaredoxin 1; macrophages; redox; thiols

Introduction

Recruitment of monocyte-derived macrophages (MDM) to sites of tissue injury is a hallmark of acute inflammation [1]. The extent of monocyte recruitment and macrophage

accumulation is generally believed to be controlled by local inflammatory processes within that tissue [2, 3]. Macrophage activation and polarization plays a critical role in both inflammation and subsequent inflammation resolution. Dysregulation of macrophage activation and plasticity has been proposed to play a major role in impaired inflammation resolution, and in the conversion of local acute inflammation into a chronic process [4]. It is now well-established that metabolic disorders, including hyperglycemia and hyperlipidemia, induce monocyte reprogramming and dysfunction [5–8]. The functional changes observed in monocytes reprogrammed by high-calorie diets (HCD) include altered gene activation profiles in response to proinflammatory and inflammation resolving stimuli and hypersensitivity to chemoattractant and accelerated chemotaxis, resulting in increased recruitment of dysfunctional MDM to sites of inflammation and accelerated atherosclerosis [9–13].

The molecular mechanisms underlying monocyte reprogramming by HCD and the associated functional changes involve the increased formation of reactive oxygen species (ROS), oxidation of reactive protein thiols to sulfenic acids, resulting in increased protein *S*-glutathionylation, the reversible formation of mixed disulfides between the cysteine of glutathione and redox-sensitive thiols on protein cysteines [14–16]. *S*-Glutathionylation can lead to the inactivation of enzymes and the degradation of proteins [17–20]. A critical target of HCD-induced protein *S*-glutathionylation in macrophages is MAPK phosphatase 1 (MKP-1), which acts as a counter-regulator of the MAPK pathways that control monocyte adhesion and migration, and thus the recruitment of MDM into tissues [21]. *S*-Glutathionylation of MKP-1 inactivates the enzyme and promotes its degradation [18], resulting in the hyperactivation of p38 and ERK pathways in response to chemokine stimulation, and thereby enhanced monocyte adhesion and chemotaxis and accelerated atherogenesis [12]. MKP-1 not only controls monocyte adhesion and chemotaxis [11] but also regulates macrophage activation, autophagy and apoptosis and controls their phenotypic fate [21]. Using a redox proteomics approach and HCD-fed atherosclerosis-prone LDL receptor-deficient mice, our group identified over 100 macrophage proteins that are *S*-glutathionylated in response to HCD-feeding [22], suggesting that exposure of blood monocytes to HCD leads to a major reprogramming of the monocyte/macrophage proteome after HCD exposure [23].

Protein *S*-glutathionylation is a reversible post-translational modification and thus represents a major redox signaling mechanism that plays a critical role in regulating monocyte and macrophage functions [10, 11, 15, 17, 19]. In mammalian cells and tissues, the reduction, i.e. "*deglutathionylation*" of protein-glutathione (GSH) mixed disulfides is catalyzed by a family of thiol transferases called glutaredoxins (Grx). During the reduction of protein-GSH mixed disulfides by Grx, a GSH molecule is transferred from the protein thiol onto the Grx molecule, forming a mixed disulfide. Free GSH selectively recycles oxidized Grx into the reduced enzyme, generating glutathione disulfide (GSSG) in the process, which in turn is reduced to two molecules of GSH by glutathione reductase (GR) [49]. Together, Grx and glutathione reductase form a unique protein thiol regulation and regeneration system distinct from the GSH-independent thioredoxin/thioredoxin reductase system [24]. The GSH/GR/Grx system plays a critical in maintaining the (thiol) redox balance of macrophages thereby protecting macrophages against dysfunction and cell death [5, 25].

Two isoforms of human Grx have been isolated and characterized, Grx1 [50] and Grx2, which shows 36% sequence identity to Grx1 [51]. Grx1, is localized primarily in the cytosol and the intermembrane space of mitochondria [26].

Our most recent data demonstrate that Grx1 deficiency sensitizes monocytes and macrophages to nutrient stress-induced dysfunction and reprogramming, accelerating diet-induced obesity, metabolic syndrome, hyperglycemia, insulin resistance and atherosclerosis [5]. Here we tested the hypothesis that overexpression of Grx1 restricted to monocytes and macrophages protects atherosclerosis-prone LDL receptor deficient mice against HCD-induced monocyte dysfunction and macrophage reprogramming, and thereby reduces the severity of atherosclerosis.

Methods

Animals and Diets

LDL-R$^{-/-}$ (B6.129S7-*Ldlr*^{tm1Her}/J, stock number 002207) and C57BL/6J (stock number 000664) were obtained from Jackson Laboratory. All mice were maintained in colony cages on a 12 h light/12 h dark cycle and fed a normal mouse laboratory diet unless otherwise stated. Four weeks after BMT, BM recipient mice were switched to either a maintenance diet (MD, AIN-90G, Bio-Serv) or a high-calorie diet (HCD; 21% milk fat wt/wt and 0.2% cholesterol wt/wt. diet no. F55440, Bio-Serv) for 20 weeks. Body weights were measured weekly. All studies were performed in accordance with the guidelines and regulations of and with the approval of the Wake Forest School of Medicine Institutional Animal Care and Use Committee.

Lentivirus Transduction of Hematopoietic Progenitor Cells

The CD68 promoter construct, which contains the 83-bp first intron (IVS-1) of the human CD68 gene [27], was kindly provided by Dr. David Greaves, University of Oxford. CD68-IRES-EGFP in pcDNA3.1 vector was digested *Cla*I/*Not*I and inserted into the corresponding site in the pRRL.cPPT.PGK-GFP.WPRE.Sin-18 backbone (Addgene), replacing the hPGK promoter and EGFP region. Lentiviruses were produced by transfecting the vector into HEK293T cells using a lentivirus packaging kit (Origene) and then concentrated with the Lenti Concentrator (Origene). Bone marrow cells were harvested from the femurs of male or female 10-week-old C57Bl6/J mice, and hematopoietic progenitor cells were isolated by negative selection using a Robosep automated cell separator (Stem Cell Technologies) and the Mouse Hematopoietic Progenitor Cell Isolation Kit (Stem Cell Technologies). Isolated cells were resuspended in RPMI supplemented with 1% Penicillin/Streptomycin, stem cell factor (100 ng/ml), Flt-3L (100 ng/ml), IL-11 (100 ng/ml) and IL-3 (20 ng/ml) and transduced with the lentiviruses (MOI = 30) by incubating overnight at 37°C in a CO_2 incubator.

Irradiation and Bone Marrow Transplantation.

Bone marrow transplantations (BMT) were conducted as described previously [28]. Briefly, two weeks before irradiation and BMT, 10-week-old male and female LDLR$^{-/-}$ mice (n=35) were put on acidified water containing sulfamethoxazole (160 ng/ml) and trimethoprim (32

ng/ml). All designated transplant recipient mice were irradiated with 2 equal doses of 4.7 Gy, with 3 h between each dose (9.4 Gy total, GammaCell Irradiator). Animals were allowed a 4 h recovery period prior to BMT. The transduced hematopoietic progenitor cells were washed with PBS and resuspended at the concentration of 5×10^5 cells/100μl. BM recipient mice were randomized into two groups based on the strain of their donors ($EGFP_{Mac}^{tg}$: 6 males, 9 females; $Grx1_{Mac}^{tg}$: 9 males, 12 females) and were injected with virus-transduced cells of the corresponding sex via the retro-orbital sinus. Animals reconstituted with the cells expressing CD68-EGFP were designated as $EGFP_{Mac}^{tg}$ and those that received CD68-Grx1-IRES-EGFP as $Grx1_{Mac}^{tg}$. BM recipients were fed a maintenance diet (MD) and allowed to recover for 4 weeks prior to initiating HCD feeding. Due to dermatitis and weight loss, 2 mice from the $EGFP_{Mac}^{tg}$ group had to be prematurely euthanatized and were excluded from the study. Complete blood counts were performed in all animals 20 weeks after BM transplantation at the time of euthanasia.

In Vivo Matrigel Chemotaxis Assay

Each mouse received two Matrigel plugs three days prior to euthanasia as described in [9, 29]. Briefly, subcutaneous injections of Matrigel (BD Biosciences) were made on the right and left flank of each mouse, one plug containing MCP-1 (500 ng/ml) and the other plug containing vehicle. After euthanasia, plugs were surgically removed, cleaned and digested with dispase (BD Biosciences). Cells were stained with Calcein/AM (Invitrogen) and counted using an automated fluorescent cell counter (Nexcelcom Bioscience).

Analysis of Atherosclerosis

Two distinct vascular beds were used for the quantification of atherosclerosis, which was conducted as described previously [9, 12, 28]. After euthanasia, hearts and aortas were perfused with phosphate-buffered saline through the left ventricle. Hearts were separated from the aorta and embedded in Tissue-Tek Optimal Cutting Temperature compound (OCT) in a plastic cryomold (Tissue-Tek). OCT-embedded hearts were rapidly frozen on dry ice and then stored at - 80°C until further processing. For *en face* analysis, aortas were dissected from the proximal ascending aorta to the bifurcation of the iliac artery and fixed with 4% paraformaldehyde in PBS. Adventitial fat was removed, and aortas were opened longitudinally and stained with Oil Red O. Stained aortas were pinned flat onto a black Sylgard layed dissection dish (Living Systems), and digitally photographed at a fixed magnification. Total aortic area and lesion areas were calculated using Image-Pro Plus (Media Cybernetics). The aortic roots from OCT-embedded hearts were sectioned every 10 μm on 8 different Superfrost Plus Gold Slides (Fisherbrand). Sections on the same slide were separated by 80 μm. Sections were stained with Oil Red O, and examined under a light microscope (Leica) with an attached digital camera. Aortic lesion areas were quantified by averaging the total lesion area across 10 sections using Image-Pro Plus (Media Cybernetics) and expressed as mm^2. To measure macrophage content in lesions, aortic root sections adjacent to the Oil Red O-stained sections were dried overnight and fixed in ice-cold 100% methanol. Fixed aortic root sections were blocked with 5% BSA (with 0.3% Triton-X100) and stained for 1 h at RT with an anti-CD68 antibody (Bio-Rad) and the nuclear stain DAPI (Invitrogen). Images were captured using a fluorescent microscope (Leica) and a high-resolution digital camera (Olympus). Macrophage content was calculated for each

cryosection using Image-Pro software and expressed as mm^2. Non-specific staining was assessed by omitting the primary antibody.

FACS Analysis

To evaluate transduction efficiency and cell specificity, EGFP expression was analyzed in white blood cells (WBC) by FACS. Whole blood was collected from the facial vein and red blood cells were lysed using RBC lysis buffer (eBioscience). WBC were stained in PBS with 1% FBS for 20 min on ice with PE-labeled anti-CD11b (eBioscience, clone: M1/70) and APC-labeled anti-Ly6G (BD, clone: 1A8). The cell suspensions were analyzed using an Accuri C6 Plus flow cytometer (BD) and the gating of the cells were performed using single-color fluorochromes. FACS data analyzed using FCS Express (De Novo Software).

Plasma Cholesterol and Triglycerides

Mice were fasted overnight prior to euthanasia and blood was collected by cardiac puncture. Plasma total cholesterol and triglycerides were quantified using enzymatic assay kits per manufacturer's protocol (Wako Chemicals USA).

Bone Marrow-Derived Macrophage Isolation and Culture

To generate BMDM, bone marrow was extracted from tibia and femur bones using aseptic technique following removal of the surrounding muscle. To do so, joints were cut using a scalpel and the exposed bone marrow was flushed out the ends of the bones using a 25-gauge needle and a 10 ml syringe filled with RPMI with 2% FBS. The cell suspension was centrifuged at 250×g for 5 min to pellet cells. The supernatants were discarded, and cells were resuspended in 1mL of RPMI (10% FBS). 500,000 cells/ml were seeded into non-tissue culture treated in RPMI 10% FBS in the presence of 50 ng/ml macrophage colony-stimulating factor (M-CSF, PeproTech). Cells were used 6–8 days after harvesting.

MKP-1 Activity

The MKP-1 activity in blood monocytes was measured as described previously [12]. Briefly, phosphatase activity, measured as inorganic phosphate released from a phosphotyrosine peptide (200 μM PTP, Millipore) was measured from cell lysates in the presence or absence of MKP-1 inhibitor (40 μM sanguinarine chloride, Tocris). The amount of inorganic phosphate released was assayed spectrophotometrically using a VersaMax spectrophotometric plate reader (Molecular Devices). Sanguinarine-sensitive phosphate released by MKP-1 was quantified with a standard curve prepared with known amounts of KH_2PO_4 (Malachite Green Assay, Cayman Chemical).

Gene Expression Analysis

Total RNA was isolated from bone marrow-derived macrophages using PureLink RNA mini kit (Invitrogen). Isolated total RNA was quantified using a Nanodrop (Thermo Fisher), and 1 ug was treated with DNase I (Invitrogen) followed by being reverse-transcribed into cDNA using SuperScript IV VILO (Invitrogen), according to manufacturer's instructions. Preamplified cDNA (100 ng) was mixed with TaqMan™ Fast Advanced Master Mix (Applied Biosystems). Thermal cycling was performed using the ViiA™7 real-time PCR

system (Applied Biosystems). The following TaqMan™ primers were used: Grx1 (*Glrx*, Mm00728386_s1), Nox4 (Mm00479246_m1), and Mao A (Mm00558004_m1). Relative gene expression was determined using the comparative ΔC_T method by comparing the C_T values of a target gene for each sample with the indicated housekeeping genes (*Rn18S, Hprt,*).

Gene profiling by quantitative real-time PCR was performed using custom-designed TaqMan® Array Cards, 384-format (Thermo Fisher). Preamplified cDNA (100 ng) was mixed with TaqMan™ Fast Advanced Master Mix (Applied Biosystems). Thermal cycling was performed using the ViiA™7 real-time PCR system (Applied Biosystems). Relative gene expression was determined using the comparative ΔC_T method by comparing the C_T values of a target gene for each sample with the housekeeping gene (*Rn18S*). ΔC_T values for each gene in BMDM from $EGFP_{Mac}$ and $Grx1_{Mac}$ LDLR-deficient mice were normalized to the mean ΔC_T value obtained for that gene in BMDM from MD-fed C57BL/6 mice. Heatmaps were generated using web-based software, Morpheus (https://software.broadinstitute.org/morpheus).

Western Blot Analysis

BMDM were washed with warm PBS and lysed on ice cold RIPA lysis buffer (50 mmol/l Tris-HCL (pH 7.5), 150 mmol/l NaCl, 1% NP-40, 0.1% SDS, 0.5 % sodium deoxycholate) supplemented with protease inhibitors (Roche). Total protein content in cell lysates was quantified by BCA assay (Pierce). Aliquots with equal amounts of protein were loaded and separated on SDS-PAGE gels. Proteins were transferred to PVDF membranes (BioRad) and probed using specific primary antibodies as follows; Grx1 (Novus), anti-GSH (Millipore), and β-actin (Cell Signaling). The bands were detected by chemiluminescence on Azure 600 (Azure Biosystems).

Statistical Analyses

Analysis of variance (ANOVA) followed by the Fisher's Least Significant Difference test was used to compare the mean values between the experimental groups (SigmaPlot 15 software). Unless stated differently, data are expressed as mean ± standard error of the mean (SEM). $P<0.05$ was set as the statistical significance level.

Results

Macrophage-restricted overexpression of Grx1 in mice protects against atherogenesis.

To determine the role of Grx1 in monocytes and macrophages on the development and progression of atherosclerosis, we generated atherosclerosis-prone male and female LDL receptor-deficient transgenic mice that overexpress either EGFP alone or both EGFP and Grx1 under the control of the macrophage-specific CD68 promoter ($EGFP_{Mac}$ and $Grx1^{tg}_{Mac}$ mice). We fed these mice either a low-calorie maintenance diet (MD) or a Western-style high-calorie diet (HCD) for 20 weeks. To verify transgene expression, RT-qPCR analysis and Western blot analysis were carried out in bone marrow-derived macrophages. We observed a 6.0-fold and a 2.8-fold increase in Grx1 mRNA levels (Fig. 1A) in male and female $Grx1^{tg}_{Mac}$ mice respectively. The increase of Grx1 mRNA

levels in female macrophages resulted in a 2.8-fold increase in Grx1 protein expression (Supplemental Fig. 1A+B). FACS analysis in these mice showed that >85% of blood monocytes expressed EGFP and that transgene expression was restricted to monocytes and granulocytes and only to a small extent to lymphocytes (<4%, not shown). To assess changes in Grx1 activity in macrophages, we used Western blot analysis to compare total protein *S*-glutathionylation levels in BMDM isolated from female HCD-fed $EGFP_{Mac}$ control mice with those in BMDM from the corresponding $Grx1^{tg}_{Mac}$ mice. Metabolic stress-induced protein *S*-glutathionylation in BMDM from HCD-fed $EGFP^{tg}_{Mac}$ control mice was reduced by 57% in BMDM isolated from $Grx1^{tg}_{Mac}$ mice (Supplemental Fig. 1C+D), confirming that Grx1 activity was significantly increased in monocytes and macrophages from transgenic $Grx1^{tg}_{Mac}$ mice.

Atherosclerotic lesion size determined by *en face* analysis of the aortic arch and the entire aorta revealed that male and female $Grx1^{tg}_{Mac}$ mice showed a 55% and 44% reduction in plaque size, respectively, compared to male and female $EGFP_{Mac}{}^{tg}$ mice (Fig. 1B). To confirm these findings, we also analyzed atherosclerotic plaque size in the aortic root of these mice. Serial analysis of ORO-stained sections from the aortic root showed a 72% and 39% decrease in atherosclerotic lesion size in male and female $Grx1_{Mac}{}^{tg}$ mice, respectively, compared to the corresponding $EGFP_{Mac}{}^{tg}$ mice (Fig 1C). Macrophage content in the vessel wall was equally strongly reduced, by 61% in male and by 40% in female mice (Fig 1D). However, heart, liver, kidney, and adipose tissue weights were not affected by Grx1 overexpression (Fig. S2A–D). We also did not observe any difference in body weight between $EGFP_{Mac}{}^{tg}$ and $Grx1_{Mac}{}^{tg}$ mice in either males (33.2 ± 2.4 g versus 34.4 ± 2.2 g) or females (32.3 ± 1.7 g versus 32.8 ± 1.1 g). Plasma total cholesterol and plasma triglyceride levels were not different either between $EGFP_{Mac}{}^{tg}$ and $Grx1_{Mac}{}^{tg}$ mice in either males (cholesterol: 893 ± 353 mg/dl versus 757 ± 125 mg/dl; triglycerides 551 ± 123 mg/dl versus 421 ± 98 mg/dl) or females (922 ± 402 mg/dl versus 1107 ± 298 mg/dl; triglycerides 454 ± 71 mg/dl versus 510 ± 134 mg/dl). Together, these findings suggest that increasing Grx1 activity in monocytes and macrophages protects mice against HCD-induced atherogenesis by reducing the recruitment of MDM to sites of vascular injury, without altering plasma lipid levels.

Macrophage-restricted overexpression of Grx1 in mice prevents MKP-1 inactivation induced by nutrient stress and the overrecruitment of monocyte-derived macrophages in HCD-fed mice.

MKP-1 is a master regulator of monocyte and macrophage activation and function which, in response to HCD-induced nutrient stress, is *S*-glutathionylated, inactivated and subsequently degraded [21]. MKP-1 deficiency in blood monocytes induced either by HCD feeding or genetically by transplanting bone marrow from MKP-1 knockout mice, promotes monocyte hyperresponsiveness to chemokines, the overrecruitment of MDM and accelerates atherogenesis in mice [18, 30]. To elucidate the molecular mechanism underlying the atheroprotective effect of monocytic Grx1 activity, we therefore examined whether increased Grx1 expression in monocytes and macrophages prevents nutrient stress-induced MKP-1 inactivation and normalizes their chemotactic activity. To this end, we measured MKP-1 activity in BMDM isolated from $EGFP_{Mac}{}^{tg}$ and $Grx1_{Mac}{}^{tg}$ mice after 20 weeks of HCD-

feeding and compared these to MKP-1 activity levels in BMDM from low-calorie MD-fed mice. MKP-1 activity was reduced by 56% in male $EGFP_{Mac}{}^{tg}$ mice and by 61% in females (Fig. 2A+B, red symbols). Overexpression of Grx1 restored monocyte MKP-1 activity to 70% in males and 67% in females relative to the MKP-1 activity measured in the respective healthy MD-fed mice (Fig. 2A, green versus gray symbols). To determine whether partially restored MKP-1 activity would also normalize the chemotactic activity of blood monocytes *in vivo* and reduce the recruitment of MDM, we conducted Matrigel plug assays [29] in all these mice. Indeed, compared to their respective $EGFP_{Mac}{}^{tg}$ mice, male $Grx1_{Mac}{}^{tg}$ mice showed a 74% reduction in MDM recruitment and females a 61% reduction (Fig. 2B), indicating increased Grx1 activity protects blood monocytes against nutrient stress-induced dysfunction and accelerated chemotactic activity.

Macrophage-restricted overexpression of Grx1 in mice partially reverses nutrient-stress induced macrophage reprogramming.

HCD-feeding of mice results in the reprogramming of their macrophages [5–8, 13, 31], although the full extent of reprogramming only becomes apparent upon macrophage polarization into proinflammatory and inflammation resolving phenotypes [30]. In agreement with our previous reports [13], in the absence of polarizing stimuli, we found that only a small percentage of macrophage genes are significantly altered in their expression, i.e. increased or decreased more than 2-fold, by HCD feeding (Fig. 3). Of the 316 genes probed, in macrophages from male mice only 57 genes showed a more than 2-fold induction and 41 showed more than 2-fold suppression, whereas macrophages from female mice showed more than a 2-fold induction of only 43 genes and a more than 2-fold suppression of 43 genes (Fig. 3B+C). The majority of gene expression changes were observed in the group of polarization makers, and in genes involved in glucose and glutamine synthesis, transport and metabolism. However, there was a large sex difference in the macrophage genes affected by reprogramming. The most profound changes were observed in the induction of NADPH oxidases and NO synthases by HCD feeding. The largest expression changes were observed for Nox2 (2.1-fold), Nox4 (10.7-fold), Nos1 (10.0-fold), Nos2 (7.8-fold) and Nos3 (2.4-fold) in male macrophages and Nox4 (4.2-fold), Nos1 (5.3-fold) and Nos3 (13.2-fold) in female macrophages, confirming sex differences in macrophage gene expression in response to HCD feeding we reported previously [5].

Of all significantly induced (94) or suppressed genes (77), only 7 genes were common to both males and females in either category, indicating major sexual difference in mice in the responses of macrophages to HCD feeding. Surprisingly, overexpression of Grx1 in macrophages only partially reversed these expression changes. Of the 84 genes significantly affected by HCD feeding in male macrophages and the 71 genes in female mice, Grx1 overexpression restored expression of only 19 genes in both males and females to levels measured in MD-fed control mice. These results suggest, that the potent atheroprotective effects of Grx1 overexpression in macrophages may not (primarily) be exerted at the transcriptional level, but rather by preventing posttranslational modifications, i.e. protein *S*-glutathionylation (Supplemental Fig. 1C+D), which can promote enzyme inactivation, protein degradation and the reprogramming of the macrophage proteome [14, 23].

Discussion

Grx1 is a thiol transferase, which specifically catalyzes the reduction of mixed disulfides between glutathione (GSH) and protein thiols [15, 17]. The formation of these mixed disulfides, referred to as "protein *S*-glutathionylation", is a reversible post-translational modification of cysteine residues, and represents a major redox signaling mechanism that play a critical role in regulating monocyte and macrophage functions [5, 10, 11, 15, 17, 19]. We showed that overexpressing Grx1 protects against metabolic stress-induced protein *S*-glutathionylation and completely prevents monocyte "priming" and dysfunction by metabolic stress *in vitro* [10, 32]. We also showed that loss of monocytic Grx1 activity disrupts the immunometabolic balance in mice and derepresses sexually dimorphic oxidative stress responses in macrophages, i.e., the differential expression of NO synthetases and NADPH oxidases in male and female monocytes and macrophages [5]. Here we now demonstrated that macrophage-restricted overexpression of Grx1 protects LDL receptor-deficient ($LDLR^{-/-}$) mice against atherosclerosis (see **Graphical Abstract**). Our findings are in good agreement with gene-disease association data from the Comparative Toxicogenomics Database (CDT) in the Harmonize database, which suggest a strong association of *Glrx1* with atherosclerosis and heart disease [33].

To elucidate the molecular mechanisms underlying the protective effect of macrophage-restricted overexpression of Grx1, we examined whether increasing Grx1 activity in macrophages would restore the transcription profile of macrophages dysregulated by HCD feeding. We conducted transcriptional profiling using our custom-designed TaqMan® Array Cards and confirmed our previous data on the sexual dimorphic expression profile of NADPH oxidases and NO synthases in male and female macrophages in response to HCD feeding [5]. We also confirmed that, with the exception of Nox2 in male macrophages, induction of NOX and NOS expression was reversed in macrophages isolated from $Grx1_{Mac}$ mice, suggesting that increasing Grx1 activity protects macrophages not only by reversing oxidative "damage", i.e. protein *S*-glutathionylation and degradation, but also indirectly by suppressing HCD-induced ROS and RNS production. Surprisingly, of the macrophage genes significantly affected by HCD-exposure, 84 in male and 71 in female mice, only a small fraction, 23% and 27%, respectively, were restored to the level found in mice fed a low-calorie MD diet. These findings suggest that while induction of ROS and RNS may be essential for HCD-induced monocyte priming and macrophage dysfunction, transcriptional reprogramming is not the sole mechanism underlying HCD-induced macrophage reprogramming and dysfunction. Posttranslational modifications of key macrophage proteins induced by HCD feeding, such as protein *S*-glutathionylation, may also have a profound and lasting impact on macrophage function, and thus on vascular inflammation and atherogenesis.

Induction and activation of NOX and NOS is likely an early event in HCD-induced macrophage dysfunction and reprogramming. We reported previously that in THP-1 monocyte-like cells, metabolic stress induced by high concentrations of glucose plus native human LDL (HG+LDL) induces Nox4 expression, H_2O_2 formation and actin *S*-glutathionylation and increases their sensitivity to MCP-1 induced chemotaxis [10]. Overexpression of Nox4 mimicked these effects whereas Nox4 knockdown or

overexpression of Grx1 reversed these effects, supporting the hypothesis that induction and activation of NOX and NOS is an early and necessary event in HCD-induced macrophage reprogramming and dysfunction. Increased production of ROS and RNS in response to nutrient stress likely also accounts for the increase in protein *S*-glutathionylation we observed in macrophages isolated from HCD-fed atherosclerosis-prone $LDLR^{-/-}$ mice [23]. Our redox proteomics data revealed that over 100 macrophage proteins are *S*-glutathionylated in response to HCD-feeding. Because *S*-glutathionylation can lead to the activation [34] or inactivation of enzymes [11, 19], and in some cases their degradation [18–20], the scale of protein *S*-glutathionylation that occurs in macrophages in response to HCD feeding suggest a major reprogramming of the macrophage proteome. Indeed, here we confirmed that HCD feeding leads to a major increase in protein S-glutathionylation in macrophages, which is prevented in mice overexpressing Grx1 in monocytes and macrophages. This finding further supports our hypothesis that HCD-induced *S*-glutathionylation and subsequent reprogramming of the macrophage proteome is an early and required step in atherogenesis. Together with our previous findings that hematopoietic overexpression of glutareductase is sufficient to protect mice against HCD-induced atherogenesis demonstrates a central role for the GSH-dependent antioxidant system in protecting macrophages from HCD-induced oxidative stress, dysfunction and reprogramming.

The redox-regulated phosphatase, MKP-1, is central to macrophage biology as this enzyme regulates signaling, polarization, functions and survival [21]. Deletion of MKP-1 mimics the effect of HFD on macrophages, promoting monocyte priming and dysfunction, macrophage reprogramming and dysregulation and accelerating atherogenesis [12, 18]. Under conditions of oxidative stress, MKP-1 is *S*-glutathionylated on the active site cysteine and subsequently degraded. Overexpression of Grx1 preserved MKP1 activity in macrophages from HCD-fed $Grx1_{Mac}$ mice, suggesting that maintaining MKP-1 activity in macrophages is likely the main mechanism by which increased Grx1 activity in macrophages prevents atherogenesis in mice. By preserving MKP-1 activity, monocyte responsiveness to chemokines is normalized as evidenced by reduced MDM accumulation in MCP-1-loaded Matrigel plugs. Reduced recruitment of MDM in turn explains the reduction of macrophage content in aortic lesions, which likely contributed to reduced plaque size in $Grx1_{Mac}$ mice. Furthermore, we showed previously that loss of MKP-1 activity enhances the polarization of macrophages into pro-inflammatory or “M1” phenotypes and dampens their conversion into an inflammation-resolving or “M2” phenotypes [12]. Thus, by preserving MKP-1 activity, overexpression of Grx1 not only limits the number of MDM recruited into atherosclerotic lesion but also restores their potential to convert into inflammation resolving macrophages.

In summary, our studies demonstrated a critical role for monocytic Grx1 in protecting against atherosclerosis. The two main mechanisms underlying the atheroprotective effects of this thiol transferase involve suppressing the expression of ROS and RNS-generating enzymes and maintaining the thiol redox state of the proteome in these cells. Our findings also suggest that intervention strategies aimed at increasing Grx1 activity may be of significant therapeutic value in the prevention and possibly the treatment of atherosclerosis. Our recent report linking HDAC2 inhibition to increased Grx1 expression and activity in macrophages supports this concept [35].

Supplementary Material

Refer to Web version on PubMed Central for supplementary material.

Financial Support

This project was supported by grants to R.A. from the NIH (HL115858 and HL153120).

Abbreviations:

BM	Bone marrow
BMDM	Bone marrow-derived macrophages
BMT	Bone marrow transplantation
FBS	Fetal bovine serum
GR	Glutathione reductase
Grx1	Glutaredoxin 1
GSH	Glutathione
HCD	High-calorie diet
MDM	Monocyte-derived macrophage
MCP-1	Monocyte chemoattractant protein-1
MD	Maintenance diet
MKP-1	Mitogen-activated protein kinase phosphatase 1
MOI	Multiplicity of Infection
RNS	Reactive nitrogen species
ROS	Reactive oxygen species

References

1. Ryan GB and Majno G, Acute inflammation. A review. Am J Pathol, 1977. 86(1): p. 183–276. [PubMed: 64118]
2. Glass CK and Witztum JL, Atherosclerosis. the road ahead. Cell, 2001. 104(4): p. 503–516. [PubMed: 11239408]
3. Ley K, et al. , Getting to the site of inflammation: the leukocyte adhesion cascade updated. Nat. Rev. Immunol, 2007. 7(9): p. 678–689. [PubMed: 17717539]
4. Ariel A, et al. , Macrophages in inflammation and its resolution. Front Immunol, 2012. 3: p. 324. [PubMed: 23125842]
5. Ahn YJ, et al. , Glutaredoxin 1 controls monocyte reprogramming during nutrient stress and protects mice against obesity and atherosclerosis in a sex-specific manner. Nat Commun, 2022. 13(1): p. 790. [PubMed: 35145079]
6. Zhang X, et al. , Reprogramming tumour-associated macrophages to outcompete cancer cells. Nature, 2023.

7. Rasheed A and Rayner KJ, Macrophage Responses to Environmental Stimuli During Homeostasis and Disease. Endocr Rev, 2021. 42(4): p. 407–435. [PubMed: 33523133]
8. Russo S, et al. , Meta-Inflammation and Metabolic Reprogramming of Macrophages in Diabetes and Obesity: The Importance of Metabolites. Front Immunol, 2021. 12: p. 746151. [PubMed: 34804028]
9. Qiao M, et al. , Thiol Oxidative Stress Induced by Metabolic Disorders Amplifies Macrophage Chemotactic Responses and Accelerates Atherogenesis and Kidney Injury in LDL Receptor-Deficient Mice. Arterioscler. Thromb. Vasc. Biol, 2009. 29: p. 1779–1786. [PubMed: 19592463]
10. Ullevig S, et al. , NADPH Oxidase 4 Mediates Monocyte Priming and Accelerated Chemotaxis Induced by Metabolic Stress. Arterioscler Thromb Vasc Biol, 2012. 32(2): p. 415–426. [PubMed: 22095986]
11. Kim HS, et al. , Redox regulation of MAPK phosphatase 1 controls monocyte migration and macrophage recruitment. Proc. Natl. Acad. Sci. U. S. A, 2012. 109(41): p. E2803–E2812. [PubMed: 22991462]
12. Kim HS, et al. , Monocytic MKP-1 is a Sensor of the Metabolic Environment and Regulates Function and Phenotypic Fate of Monocyte-Derived Macrophages in Atherosclerosis. Scientific Reports, 2016. 6: p. 34223. [PubMed: 27670844]
13. Ahn YJ, et al. , Dietary 23-hydroxy ursolic acid protects against diet-induced weight gain and hyperglycemia by protecting monocytes and macrophages against nutrient stress-triggered reprogramming and dysfunction and preventing adipose tissue inflammation. J Nutr Biochem, 2020. 86: p. 108483. [PubMed: 32860922]
14. Ullevig S, Kim HS, and Asmis R, S-glutathionylation in monocyte and macrophage (dys)function. Int. J. Mol. Sci, 2013. 14(8): p. 15212–15232. [PubMed: 23887649]
15. Shelton MD and Mieyal JJ, Regulation by reversible S-glutathionylation: molecular targets implicated in inflammatory diseases. Mol. Cells, 2008. 25(3): p. 332–346. [PubMed: 18483468]
16. Matsui R, et al. , Redox Regulation via Glutaredoxin-1 and Protein S-Glutathionylation. Antioxid Redox Signal, 2020. 32(10): p. 677–700. [PubMed: 31813265]
17. Shelton MD, Chock PB, and Mieyal JJ, Glutaredoxin: Role of reversible protein-S-glutathionylation and regulation of redox signal transduction and protein translocation. Antioxid. Redox Signal, 2005. 7(3–4): p. 348–366. [PubMed: 15706083]
18. Kim HS, et al. , Redox regulation of MAPK phosphatase 1 controls monocyte migration and macrophage recruitment. Proc Natl Acad Sci U S A, 2012. 109(41): p. E2803–12. [PubMed: 22991462]
19. Kim HS, et al. , Redox regulation of 14-3-3zeta controls monocyte migration. Arterioscler. Thromb. Vasc. Biol, 2014. 34(7): p. 1514–1521. [PubMed: 24812321]
20. Zetterberg M, et al. , Glutathiolation enhances the degradation of gammaC-crystallin in lens and reticulocyte lysates, partially via the ubiquitin-proteasome pathway. Invest Ophthalmol. Vis. Sci, 2006. 47(8): p. 3467–3473. [PubMed: 16877417]
21. Kim HS and Asmis R, Mitogen-activated protein kinase phosphatase 1 (MKP-1) in macrophage biology and cardiovascular disease. A redox-regulated master controller of monocyte function and macrophage phenotype. Free Radic Biol Med, 2017. 109: p. 75–83. [PubMed: 28330703]
22. Reiner JM, et al. , Analytic procedures for data on whole-body metabolism of cholesterol. Exp. Mol. Pathol, 1975. 22: p. 65–72. [PubMed: 1116567]
23. Ullevig SL, et al. , Protein S-Glutathionylation Mediates Macrophage Responses to Metabolic Cues from the Extracellular Environment. Antioxid Redox Signal, 2016. 25(15): p. 836–851. [PubMed: 26984580]
24. Lee S, Kim SM, and Lee RT, Thioredoxin and thioredoxin target proteins: from molecular mechanisms to functional significance. Antioxid Redox Signal, 2013. 18(10): p. 1165–207. [PubMed: 22607099]
25. Qiao M, et al. , Increased expression of glutathione reductase in macrophages decreases atherosclerotic lesion formation in low-density lipoprotein receptor-deficient mice. Arterioscler Thromb Vasc Biol, 2007. 27(6): p. 1375–1382. [PubMed: 17363688]

26. Pai HV, et al. , What is the functional significance of the unique location of glutaredoxin 1 (GRx1) in the intermembrane space of mitochondria? Antioxid Redox Signal, 2007. 9(11): p. 2027–33. [PubMed: 17845131]

27. Gough PJ, Gordon S, and Greaves DR, The use of human CD68 transcriptional regulatory sequences to direct high-level expression of class A scavenger receptor in macrophages in vitro and in vivo. Immunology, 2001. 103(3): p. 351–361. [PubMed: 11454064]

28. Qiao M, et al. , Increased expression of glutathione reductase in macrophages decreases atherosclerotic lesion formation in low-density lipoprotein receptor-deficient mice. Arterioscler Thromb Vasc Biol, 2007. 27(6): p. 1375–82. [PubMed: 17363688]

29. Ahn YJ, Wang L, and Asmis R, Quantification of Monocyte Chemotactic Activity In Vivo and Characterization of Blood Monocyte Derived Macrophages. J Vis Exp, 2019(150).

30. Kim HS, et al. , Monocytic MKP-1 is a Sensor of the Metabolic Environment and Regulates Function and Phenotypic Fate of Monocyte-Derived Macrophages in Atherosclerosis. Sci Rep, 2016. 6: p. 34223. [PubMed: 27670844]

31. Palsson-McDermott EM, et al. , Pyruvate kinase M2 regulates Hif-1alpha activity and IL-1beta induction and is a critical determinant of the warburg effect in LPS-activated macrophages. Cell Metab, 2015. 21(1): p. 65–80. [PubMed: 25565206]

32. Ullevig SL, et al. , Protein S-Glutathionylation Mediates Macrophage Responses to Metabolic Cues from the Extracellular Environment. Antioxid Redox Signal, 2016.

33. Rouillard AD, et al. , The harmonizome: a collection of processed datasets gathered to serve and mine knowledge about genes and proteins. Database (Oxford), 2016. 2016.

34. Adachi T, et al. , S-Glutathiolation by peroxynitrite activates SERCA during arterial relaxation by nitric oxide. Nat. Med, 2004. 10(11): p. 1200–1207. [PubMed: 15489859]

35. Wang L, Ahn YJ, and Asmis R, Inhibition of myeloid HDAC2 upregulates glutaredoxin 1 expression, improves protein thiol redox state and protects against high-calorie diet-induced monocyte dysfunction and atherosclerosis. Atherosclerosis, 2021. 328: p. 23–32. [PubMed: 34077868]

Highlights

- Macrophage-restricted Grx1 overexpression suppresses atherogenesis in LDLR−/− mice.
- Overexpression of Grx1 restores MKP-1 activity in macrophage.
- Overexpression of Grx1 normalizes recruitment of monocyte-derived macrophages.
- Grx1 overexpression partially restores gene profiles of HCD-exposed macrophages.

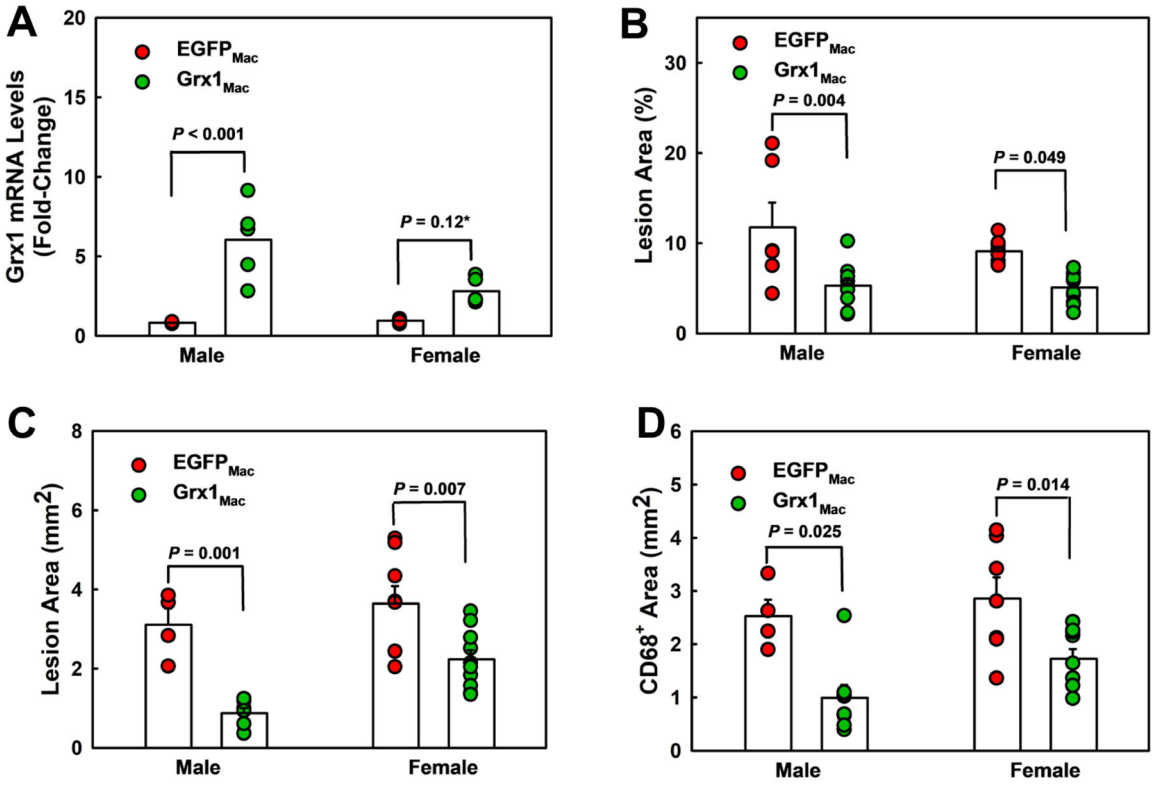

Figure 1: Macrophage-Restricted Overexpression of Grx1 Reduces Atherosclerotic Plaque Size and Macrophage Content in the Vessels.

A) Grx1 mRNA levels in BMDM isolated from 4 male and 5 female $EGFP_{Mac}^{tg}$ (•) and 5 male and 5 female $Grx1_{Mac}^{tg}$ mice fed a HCD for 20 weeks. **B**) Quantitation of the aortic lesion area. **C**) Quantitation of the lesion area in the aortic root. **D**) Quantitation of macrophage content in atherosclerotic lesions. Lesion size and macrophage content of lesions was measured in 6 male and 9 female $EGFP_{Mac}^{tg}$ (•) and 8 male and 11 female $Grx1_{Mac}^{tg}$ mice (•) after 20 weeks on HFD. All data are expressed as mean ± SEM. One-way ANOVA followed by Fisher's Least Significance Difference test was used to compare the mean values between experimental groups.

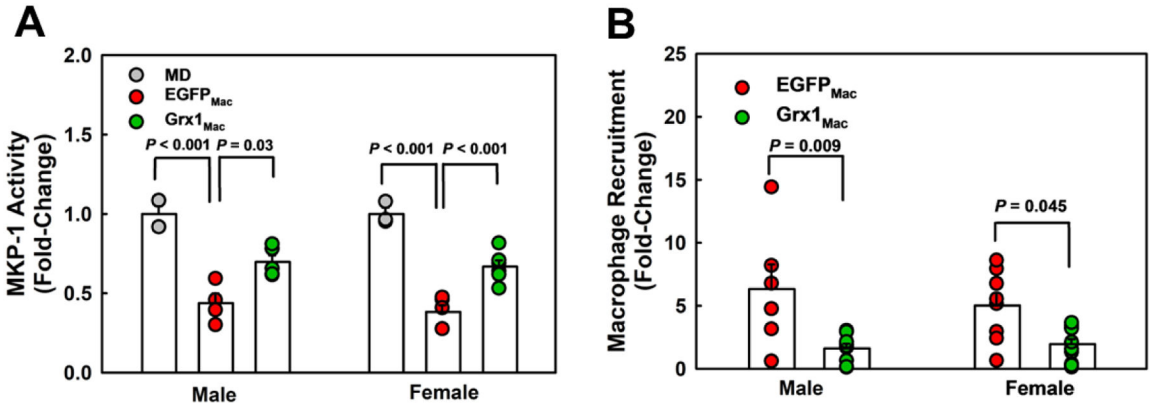

Figure 2: Overexpression of Grx1 Restores MKP-1 Activity and Reduces Monocyte Chemotaxis and Recruitment of Monocyte-Derived Macrophages

A) MKP-1 activity in BMDM isolated from 3 male and 3 female C57BL/6 mice fed a MD (•), 4 male and 5 female $EGFP_{Mac}^{tg}$ mice (•) and 5 male and 5 female $Grx1_{Mac}^{tg}$ mice (•) fed a HCD for 20 weeks. **B**) Recruitment of MDM *in vivo* determined in 6 male and 9 female $EGFP_{Mac}^{tg}$ (•) and 9 male and 11 female $Grx1_{Mac}^{tg}$ mice (•) fed a HCD for 20 weeks. Monocyte chemotaxis and MDM recruitment was determined using the Matrigel Plug assay as described in "Methods". All data are expressed as mean ± SEM. One-way ANOVA followed by Fisher's Least Significance Difference test was used to compare the mean values between experimental groups.

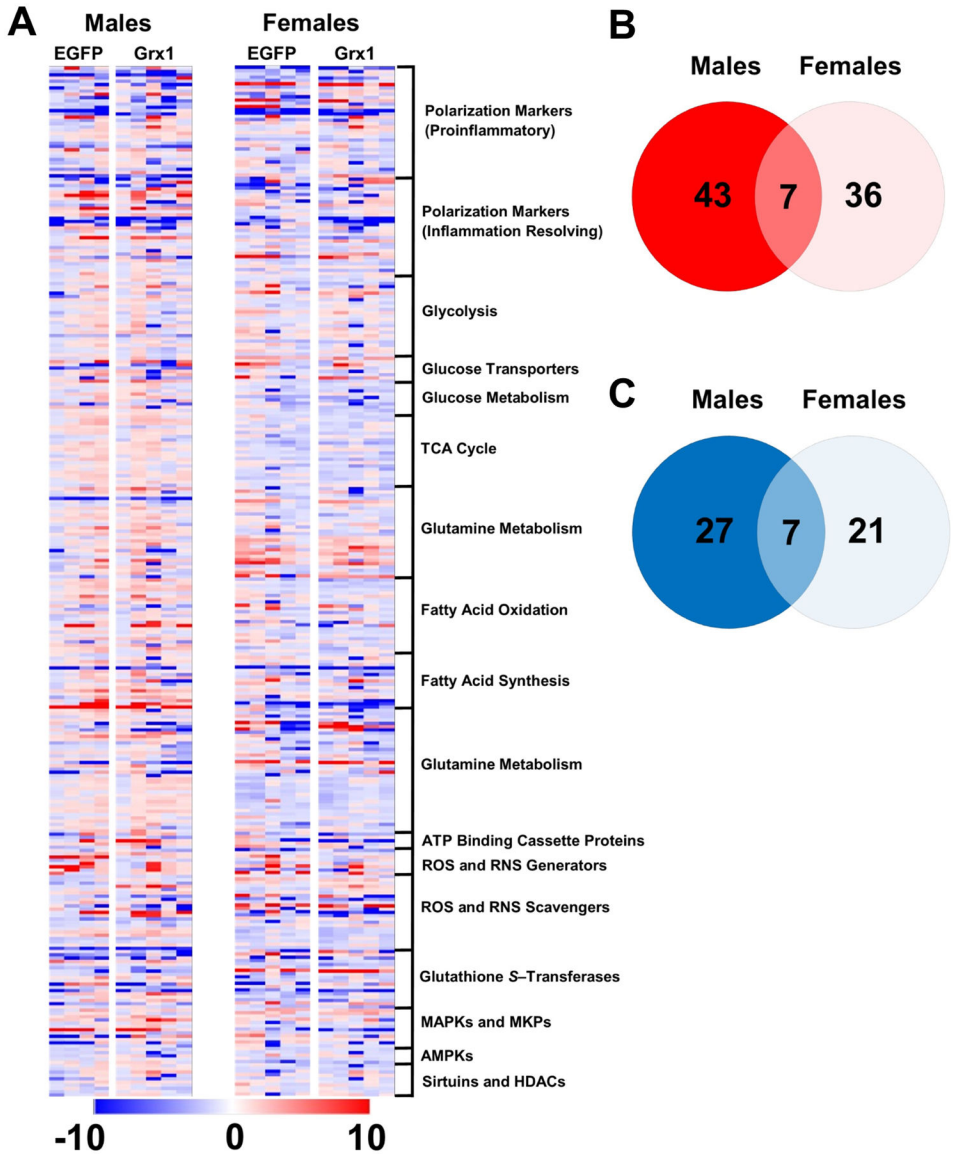

Figure 3: Grx1 Overexpression Only Partially Restores Gene Profiles Dysregulated by HCD Feeding in Macrophages Isolated from Male and Female LDLR-Deficient Mice.

A) Heat maps obtained by gene profiling conducted by qRT-PCR using custom-designed Taqman® Array Cards and mRNA isolated from BMDM from randomly selected male and female MD-fed C57BL/6 mice and HCD-fed $EGFP_{Mac}{}^{tg}$ and $Grx1_{Mac}{}^{tg}$ LDLR-deficient mice as described under “Methods”. The 316 genes were grouped by macrophage activation states and metabolic pathways (Table 1). **B+C)** Venn diagrams illustrating the number of genes in BMDM obtained from male and female $EGFP_{Mac}{}^{tg}$ mice upregulated (•,•) or downregulated (•,•) more than 2-fold by HCD feeding.

Table 1:
Target genes and primers used for targeted gene profiling by qRT-PCR.

See “Methods” for details.

Category	Gene Symbol	Assay ID
Polarization markers-Inflammatory	Myd88	Mm00440338_m1
	Arg2	Mm00477592_m1
	Ccl2	Mm00441242_m1
	Ifng	Mm99999071_m1
	Ccl9	Mm00441260_m1
	Ccr7	Mm99999130_s1
	Ccr7	Mm99999130_s1
	Ccl8	Mm01297183_m1
	Cd86	Mm00444543_m1
	Cxcl9	Mm00434946_m1
	Cxcl10	Mm00445235_m1
	Cxcl13	Mm04214185_s1
	Il1b	Mm00434228_m1
	Il6	Mm00446190_m1
	Il31ra	Mm01304496_m1
	Il17ra	Mm00434214_m1
	Ptgs2	Mm00478372_m1
	Rela	Mm00501346_m1
	Tlr2	Mm01213946_g1
	Tlr4	Mm00445273_m1
	Tnfa	Mm00443258_m1
	Cox2	Mm03294838_g1
	Stat5	Mm03053818_s1
	Irf3	Mm00516784_m1
	Irf5	Mm00496477_m1
	Nlrp3	Mm00840904_m1
	Klf6	Mm00516184_m1
	Ccl3	Mm00441259_g1
	Hif1a	Mm00468869_m1
	Stat1	Mm00439531_m1
	Stat2	Mm00490880_m1
	Pparg	Mm01184322_m1
Polarization markers-Inflammation resolving	Arg1	Mm01190441_g1
	Ccr5	Mm01963251_s1
	MIF	Mm01611157_gH
	Ccl7	Mm00443113_m1
	Cd36	Mm00432403_m1
	Cd163	Mm00474096_m1

Category	Gene Symbol	Assay ID
	Cd206	Mm01329362_m1
	Cd209a	Mm00460066_g1
	Chi3l3 (Ym1)	Mm00657889_mH
	Il10	Mm01288386_m1
	Igf1	Mm00439560_m1
	Klf4	Mm00516104_m1
	Folr2	Mm00433357_m1
	Mgl2	Mm00460844_m1
	Retnla (Fizz1)	Mm00445110_g1
	Tfrc	Mm00441941_m1
	Tgfb1	Mm01178820_m1
	COX1	Mm04225243_g1
	Ppargc1b	Mm00504720_m1
	Tfam	Mm00447485_m1
	Irf4	Mm00516431_m1
	cMyc	Mm00487804_m1
	Nrf2	Mm00477784_m1
	Stat3	Mm01219775_m1
	Stat6	Mm01160477_m1
	Hif2a (Epas1)	Mm01236112_m1
	Ppard	Mm00803184_m1
ROS & ROS generators	Nox1	Mm00549163_g1
	Cybb	Mm01287743_m1
	Nox4	Mm00479239_g1
	Mao-a	Mm00558004_m1
	Mao-b	Mm00555412_m1
	Nos1	Mm00435175_m1
	Nos2	Mm00440485_m1
	Nos3	Mm00435204_m1
GSTs	Gsta2	Mm03019257_g1
	Gsta3	Mm00494798_m1
	Gstk1	Mm00504022_m1
	Gstm1	Mm00833915_g1
	Gstm2	Mm00725711_s1
	Gstm4	Mm00728197_s1
	Gstm5	Mm00515890_m1
	Gsto1	Mm00599866_m1
	Gsto2	Mm00509763_m1
	Gstp1	Mm04213618_gH
	Gstt2	Mm00494804_g1
	Gstz1	Mm00515900_m1
	Mgst1	Mm00498294_m1

Category	Gene Symbol	Assay ID
	Mgst2	Mm00723390_m1
	Mgst3	Mm00787806_s1
Peroxiredoxins	Prdx1	Mm01621996_s1
	Prdx2	Mm04208213_g1
	Prdx3	Mm00545848_m1
	Prdx4	Mm00450261_m1
	Prdx5	Mm00465365_m1
	Prdx6	Mm07306454_mH
Gamma glutamine cysteine ligase	Gclc	Mm00802655_m1
	Gclm	Mm00514996_m1
Glutathione synthetase	Gss	Mm00515065_m1
Glutathione reductase	Gr/Gsr	Mm00439154_m1
Glrx	Grx1	Mm00728386_s1
	Grx2	Mm00469836_m1
Superoxide dismutases	Sod1	Mm01344233_g1
	Sod2	Mm01313000_m1
Catalase	Cat	Mm00437992_m1
Antioxidant System- Glutathione peroxidases	Gpx1	Mm00656767_g1
	Gpx2	Mm00850074_g1
	Gpx3	Mm00492427_m1
	Gpx4	Mm00515041_m1
	Gpx5	Mm01165467_g1
	Gpx6	Mm00513980_gH
	Gpx7	Mm00481133_m1
Glycolysis	Aldoa	Mm00833172_g1
	Aldoc	Mm01298116_g1
	Bpgm	Mm00500291_m1
	Eno1	Mm01619597_g1
	Eno2	Mm00469062_m1
	Eno3	Mm00468267_m1
	Galm	Mm01233311_m1
	Gapdh	Mm99999915_g1
	Gpi1	Mm01962484_u1
	Hk1	Mm00439344_m1
	Hk2	Mm00443385_m1
	Hk3	Mm01341942_m1
	Ldha	Mm01612132_g1
	Pfkl	Mm00435587_m1
	Pfkm	Mm01309576_m1
	Pfkp	Mm00444792_m1
	Pfkfb2	Mm00435575_m1
	Pfkfb3	Mm00504650_m1

Category	Gene Symbol	Assay ID
	Pfkfb4	Mm00557176_m1
	Pgam1	Mm02526975_g1
	Pgam5	Mm01205823_m1
	Pgk1	Mm00435617_m1
	Pkm2	Mm00834102_gH
	Tpi1	Mm00833691_g1
Glutamine metabolism	Slc1a4	Mm00444532_m1
	Slc1a5	Mm00436603_m1
	Slc3a2	Mm00500521_m1
	Slc7a5	Mm00441516_m1
	Slc7a6	Mm00626779_m1
	Slc7a7	Mm00448764_m1
	Slc38a1	Mm00506391_m1
	Slc38a2	Mm00628416_m1
	Aldh4a1	Mm00615268_m1
	Aldh18a1	Mm00444767_m1
	Asl	Mm01197741_m1
	Ass1	Mm00711256_m1
	Cad	Mm01216345_m1
	Gfpt1	Mm00600127_m1
	Pfas	Mm01325237_m1
	Ppat	Mm00549096_m1
	Glud1	Mm00492353_m1
	Glul	Mm00725701_s1
	Gls	Mm01257297_m1
	Got1	Mm01195792_g1
	Got2	Mm00494703_m1
	Gpt1	Mm00805379_g1
	Gpt2	Mm00558028_m1
	Nit2	Mm00517778_m1
	Oat	Mm00497544_m1
	Odc1	Mm01964631_g1
	Prodh	Mm00448401_m1
	Srm	Mm00726089_s1
TCA cycle	Pck2	Mm00551411_m1
	Acly	Mm01302282_m1
	Aco1	Mm00801417_m1
	Aco2	Mm00475673_g1
	Cs	Mm00466043_m1
	Dlat	Mm00455160_m1
	Dld	Mm00432831_m1
	Dlst	Mm00513470_m1

Category	Gene Symbol	Assay ID
	Fh1	Mm01321349_m1
	Idh1	Mm00516030_m1
	Idh2	Mm00612429_m1
	Idh3a	Mm00499674_m1
	Idh3b	Mm00504589_m1
	Idh3g	Mm00599686_g1
	Mdh1	Mm00485106_m1
	Mdh2	Mm00725890_s1
	Ogdh	Mm00803119_m1
	Pdha1	Mm00468675_m1
	Pdhb	Mm00499323_m1
	Sdhc	Mm00481172_m1
	Sdhd	Mm00546511_m1
	Suclg1	Mm00451244_m1
	Suclg2	Mm01182162_g1
Fatty acid oxidation	Cd36/FAT	Mm00432403_m1
	Acadl	Mm00599660_m1
	Acadvl	Mm00444293_m1
	Acadm	Mm01323360_g1
	Acads	Mm00431617_m1
	Cpt1a	Mm01231183_m1
	Fatp1/ Slc27a1	Mm00449511_m1
	Fatp3/ Slc27a3	Mm01220017_m1
	Fatp4/ Slc27a4	Mm01327405_m1
	Fabp3	Mm02342495_m1
	Fabp4	Mm00445878_m1
	Me1	Mm00782380_s1
	Sdhb	Mm00458272_m1
	Cpt	Mm00487205_m1
	Hadha	Mm00805228_m1
	Acox1	Mm01246834_m1
	Hadhb	Mm00695255_g1
	Slc25a20	Mm00451571_m1
	Hsd17b4	Mm00500443_m1
	Hadh	Mm00492535_m1
	Scp2	Mm01257982_m1
	Ehhadh	Mm00619685_m1
Fatty acid synthesis - Fatty acid desaturases	Fads1	Mm00507605_m1
	Fads2	Mm00517221_m1
	Fads3	Mm01200850_m1

Category	Gene Symbol	Assay ID
	Fads6	Mm00626150_m1
	Scd1	Mm00772290_m1
	Scd2	Mm01208542_m1
	Degs1	Mm00492146_m1
	Fexred1	Mm00549438_m1
	Fexred2	Mm01720535_m1
	Rnls	Mm04178677_m1
	Ndor1	Mm00626390_m1
	Acp/Ndufab1	Mm01137654_g1
	Dgat1	Mm00515643_m1
	Dgat2	Mm00499536_m1
	Fasn	Mm00662319_m1
Cholesterol metabolism	Hmgcs1	Mm01304569_m1
	Hmgcr	Mm01282499_m1
	Pmvk	Mm01212763_m1
	Fdft1	Mm01598574_g1
	Mvk	Mm00445773_m1
	Fdps	Mm00836315_g1
	Dhcr7	Mm00514571_m1
	Lss	Mm00461312_m1
	Sqle	Mm00436772_m1
	Ggps1	Mm00656129_mH
	Ndufa1	Mm00444593_m1
	Ndufa2	Mm00477755_g1
	Ndufa3	Mm01329704_g1
	Ndufa4	Mm00809672_s1
	Ndufa5	Mm01165335_m1
	Ndufa6	Mm01303455_g1
	Ndufa7	Mm00458227_m1
	Ndufa8	Mm00503351_m1
	Ndufa9	Mm00481216_m1
	Ndufa10	Mm00600325_m1
	Ndufa11	Mm01236867_g1
	Ndufa12	Mm01240336_m1
	Acat1	Mm00507463_m1
	Acat2	Mm00782408_s1
	Acaca	Mm01304257_m1
	Fas	Mm01204974_m1
	Srebp-1c	Mm00550338_m1
	Adrp/Plin2	Mm00475794_m1
	Etfdh	Mm01220210_m1
	Apoa1	Mm00437569_m1

Category	Gene Symbol	Assay ID
	Apoa2	Mm00442687_m1
	Apoc1	Mm00431816_m1
	Apoc2	Mm00437571_m1
	Lcat	Mm01247340_m1
	Lpl	Mm00434764_m1
	Npc1	Mm00435300_m1
	Mttp	Mm00435015_m1
	Npc2	Mm00499230_m1
Liver X receptor	Lxra	Mm00441185_m1
	Lxrb/Nr1h2	Mm00437265_g1
ATP-binding cassetts (ABC) transporters	Abca1	Mm00442646_m1
	Abcc1	Mm00456156_m1
	Abcc3	Mm00551550_m1
	Abcc4	Mm01226381_m1
Transporters	Slc2a1	Mm00441480_m1
	Slc2a3	Mm00441483_m1
	Slc2a4	Mm00436615_m1
	Slc2a6	Mm00554217_m1
	Slc2a8	Mm00444634_m1
	Slc2a9	Mm00455122_m1
	Slc2a12	Mm02375931_s1
	Slc17a5	Mm00555344_m1
Glucose metabolism	Akt1	Mm01331626_m1
	Akt2	Mm05804785_gH
	Pik3r1	Mm01282781_m1
	Ugp2	Mm00454826_m1
	Pdp1	Mm01217532_m1
	Pdp2	Mm01252669_s1
	Pdhx	Mm00558275_m1
	Pdpr	Mm01243524_m1
	Pdk1	Mm00554300_m1
	Pdk2	Mm00446681_m1
	Pdk3	Mm00455220_m1
	Pdk4	Mm01166879_m1
Transcription factors	Nfkb1	Mm00476361_m1
	Ppara	Mm00440939_m1
	Stat4	Mm00448881_m1
MKPs	Mkp-1	Mm00457274_g1
	Mkp-2	Mm00723761_m1
	Mkp-3	Mm00518185_m1
	Mkp-4	Mm00512648_g1
	Mapk8	Mm00489514_m1

Category	Gene Symbol	Assay ID
	Mapk14	Mm01301009_m1
AMPKs	Prkaa1	Mm01296700_m1
	Prkab1	Mm01201921_m1
	Prkab2	Mm01257133_m1
	Prkag1	Mm00450298_g1
	Prkag2	Mm00513977_m1
Protein kinase Cs	Prkca	Mm00440858_m1
	Prkcb	Mm00435749_m1
	Prkcd	Mm00440891_m1
	Prkci	Mm00435769_m1
	Acsf3	Mm00460721_m1
HDAC - Sirtuins	Sirt1	Mm00490758_m1
	Sirt2	Mm01149204_m1
	Sirt3	Mm00452131_m1
	Sirt4	Mm01201915_m1
	Sirt5	Mm00663723_m1
	Sirt6	Mm01149042_m1
	Sirt7	Mm01248607_m1
Histone deacetylases	Hdac1	Mm02745760_g1
	Hdac2	Mm00515108_m1
	Hdac3	Mm00515916_m1
	Hdac6	Mm00515945_m1